RSC Advances

PAPER

View Article Online
View Journal | View Issue

Cite this: *RSC Adv.*, 2019, **9**, 41319

Thermal behavior and combustion of Al nanoparticles/ MnO_2-nanorods nanothermites with addition of potassium perchlorate

Jiaxing Song,[ab] Tao Guo, *[a] Miao Yao,[a] Wen Ding,[a] Xiaonan Zhang,[a] Fengli Bei,[b] Jian Tang,[c] Junyi Huang[a] and Zhongshen Yu[a]

Received 22nd October 2019
Accepted 3rd December 2019

DOI: 10.1039/c9ra08663c

rsc.li/rsc-advances

To explore the effect of potassium perchlorate ($KClO_4$) on Al nanoparticles/MnO_2-nanorods nanothermite systems, in this paper, Al/MnO_2 nanothermites with different mass fraction of $KClO_4$ were prepared by electrospray. The samples were characterized by XRD, SEM, TG-DSC analysis. According to the results of TG-DSC, the addition of $KClO_4$ seemed to cause no direct improvement on their exothermic reactions. But the results of activation energy calculations showed that $KClO_4$ could remarkably reduce the activation energy of nanothermite systems by up to 48.8%. The XRD results indicated that residues consisted mainly of Mn_3O_4. The reasons why $KClO_4$ has little effect on thermal properties but makes a great difference on kinetics were analyzed and discussed. Finally, onset combustion tests were carried out. The results and findings provide a useful approach to decrease the activation energy and combustion rate of nanothermites, which may facilitate practical and combustible applications.

1 Introduction

With the development of nanotechnology, researchers continue to focus on nanothermites as an energetic material which usually contains both a metallic oxidizer and fuel.[1,2] It can undergo very intense redox reactions in a short period of time, which could find applications in ammunition primers,[3] nano-scale welding,[4] gas generators,[5] as well as energetic additives in both explosives and propellants.[6,7]

In the meantime, a wide variety of preparation technologies, including traditional and emerging methods, have been widely applied to nanothermite preparation and fabrication. Physical mixing is the simplest and most common method, but it has little effect on the agglomeration of nanoparticles. Hosseini and his co-authors[8] focused on the thermal and kinetic analysis of the effects of agglomeration of CuO on the Mg–CuO thermite reaction system. They prepared stoichiometric thermite mixtures by using physical mixing method and ultrasonic mixing method, and the results showed that the decrease of agglomeration could effectively reduce the activation energy. Wang[9] chose sol–gel technique to fabricate Al/Fe_2O_3 nano-composites. The results indicated that sol–gel method could let both nano-Al and micro-Al successfully wrapped by amorphous Fe_2O_3 nanoparticles. But this method has too many influencing factors, such as the amount of water, drop rate, reaction temperature and gelation process. By the way, some of those factors are pretty hard to control. Arrested reactive milling (ARM) is a versatile and useful approach to manufacture nanocomposites in industrial field while the products from ARM usually have uneven particle size distribution, irregular shape and poor flowability.[10,11] Recently, several advanced methods start to be applied into nanothermite preparation, which could achieve homogeneous mixture with more contact points between metallic oxidizer and fuel, including RF and magnetron sputtering,[12,13] cold spray,[14] thermal evaporation[15] as well as electrospray approach.[16,17]

In this work, we selected electrospray approach to prepare the samples, which could break up the liquid solution into tiny droplets by using electrostatic field forces. Usually, a high voltage is applied to the liquid in the tube through a thin glass or metal tube. A Taylor cone is formed at the end of the liquid outflow tube, and the jet thin line is formed at the end and atomized, while the droplets are rapidly released from the end of the thin line. The basis of this phenomenon is that the amount of charge that can pass through the surface of the droplet is finite, which can be broken into small droplets under the action of Coulomb Repulsive Force.[18,19]

Manganese dioxide (MnO_2) has its unique and excellent electrochemical, catalytic, environmental and also economic characteristics, which is a significant materials as battery electrode raw materials.[20] But according to famous Fischer's report,[21] MnO_2 could be a metallic oxidizer in thermite system, and theoretically its heat release is pretty high. Therefore, this

[a]College of Field Engineering, Army Engineering University of PLA, Nanjing, 210007, China. E-mail: guotao3579@126.com
[b]School of Chemical, Nanjing University of Science and Technology, Nanjing, 210094, China
[c]School of Materials Science and Engineering, Northwestern Polytechnical University, Xi'an, 710072, China

work chose MnO_2 nanorods as metallic oxidizer to combine with Al nanoparticles, as nanothermite.

Potassium perchlorate ($KClO_4$) is an important energetic additive in many pyrotechnic compositions for a long time due to its mild phase transition, moderate sensitivity and fast ignitability.[22–24] Yang and his co-authors[25] had prepared the $KClO_4$/Al/CuO nanoenergetic materials by solvent and non-solvent method. They tested the reactive pressure from electrical ignition experiments, and the results showed that $KClO_4$/Al/CuO nanoenergetic materials are more sensitive to be ignited with much higher burning rate. Clark[26] selected silicon as binder to manufacture flexible free-standing Al/MoO_3 energetic films, and to prevent the phenomenon of thermal instability, $KClO_4$ was added into the films. Besides, what needs to be pointed out is that MnO_2, as a kind of transition metal oxide, could catalyzes the decomposition of $KClO_4$, which will help release the gaseous oxygen, increase reaction rate and reduce the activation energy to some extent.[27,28]

In this work, we used electrospray approach to prepare nanothermites. At first, the MnO_2 nanorods were synthesized *via* hydrothermal method by using reactors. Then, $KClO_4$ was selected as energetic additive to add into Al nanoparticles/MnO_2-nanorods system with different mass fraction from 0% to 30%, and the thermal properties of samples were characterized, and kinetics was also calculated. Based on the results, the possible mechanism were analyzed and discussed. In the end, the onset ignition and combustion experiments were carried out to test their combustion performance.

2 Experimental

2.1 Materials

The Al nanoparticles (~100 nm) were purchased from Naiou Nano Technology Co., LTD. (Shanghai, China). $KMnO_4$ and HCl were purchased from Lingfeng Chemical Reagent Co., LTD. (Shanghai, China) to further prepare MnO_2 nanorods. $KClO_4$ as a high-energy additive was purchased by Sinopharm Chemical Reagent Co., Ltd. (Shanghai, China).

MnO_2 nanorods were synthesized *via* hydrothermal method. The chemical reaction equation is as follows:

$$2KMnO_4 + 8HCl \rightarrow 2KCl + 2MnO_2\downarrow + 3Cl_2 + 4H_2O \quad (1)$$

The amount of $KMnO_4$ should be excessive to ensure that more MnO_2 could be produced rather than $MnCl_2$. First, 1.5 g $KMnO_4$ was dissolved into 20 mL deionized water. Meanwhile, 1.875 mL HCl was diluted with 10 mL deionized water. Then, both of two solutions were mixed with intense stirring. Next, the mixture was poured into a 50 mL Teflon-lined stainless steel autoclave, sealed and maintained at 200 °C for 6 h in muffle roasting oven. When the autoclave was cooled to the room temperature, the products were taken out, which was a dark brown granule. The obtained powder was washed for several times with deionized water and ethyl alcohol, respectively. After the centrifugal operation, the product was dried at 80 °C for 12 h.

Table 1 The details of each precursor

Sample	Mass-Al/mg	Mass-MnO_2/mg	Mass-$KClO_4$/mg
I_{00}	40	60	—
II_{10}	36	54	10
III_{20}	32	48	20
IV_{30}	28	42	30

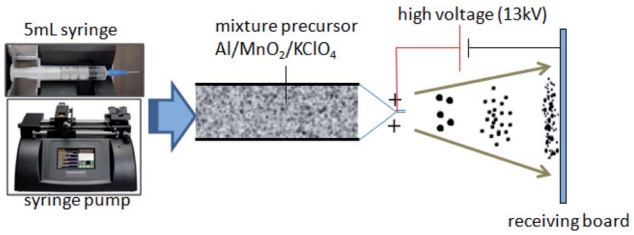

Fig. 1 Schematic diagram of electrospray process.

2.2 Precursor preparation

Each group was controlled at 100 mg. For instance, 36 mg Al nanoparticles and 54 mg MnO_2 nanorods were dispersed in 3 mL ethanol, and 10 mg $KClO_4$ was dissolved in 2 mL deionized water. Namely, the mass fraction of $KClO_4$ was 10 wt%. Then, the $KClO_4$ solution was poured into mixed turbid ethanol under intense ultrasonic conditions. Table 1 shows the details of each precursor.

2.3 Electrospray process

As shown in Fig. 1, in a typical preparation process, the mixture precursor was loaded into a 5 mL syringe with a metal flat needle, about 0.43 mm diameter. A syringe pump is introduced to eject the mixture precursor with a speed of 4.0 mL h^{-1}. The aluminum foil was set as a receiving board at 15 cm away from the syringe pump. A high voltage was applied between the needle and board, about 13 kV.

2.4 Characterization and thermal analysis

The synthesized MnO_2 nanorods and reaction products were characterized by using XRD analysis (Bruker, D8 Advance, Germany). The morphologies and particle sizes of the samples were characterized by FE-SEM analysis (HITACHI High-Technologies corporation, S-4800 II Japan).

The thermal behaviors of both components and thermite samples were carried out by using TG-DSC (NETZSCH STA 449F3, Germany). The sample mass was about 5 mg and the heating rates are 5, 10, 15, 20 °C min^{-1} in corundum crucible, covering the temperature range from room temperature to 800 °C in argon atmosphere.

3 Results and discussion

3.1 Analysis of synthesized MnO_2

In Fig. 2, the synthesized MnO_2 was analyzed by XRD. According to the tetragonal manganese oxide phase (ICDD/JCPDS 44-0141

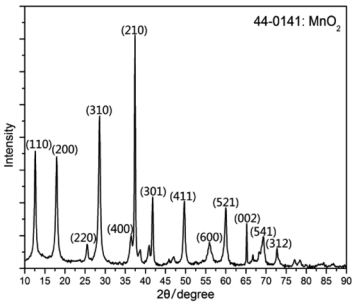

Fig. 2 XRD pattern of synthesized MnO_2.

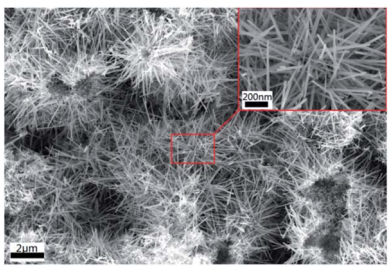

Fig. 3 FE-SEM image of synthesized MnO_2.

MDI Jade 6.0), the matching degree is pretty high, and the lattice constants are $a = b = 9.785$ Å, $c = 2.863$ Å, $c/a = 0.293$ and the space group is $I4/m$. At the same time, it can be found that there are no distinct anomalous peaks.

Fig. 3 shows the FE-SEM image of the synthesized MnO_2. The morphologies of synthesized MnO_2 are nanorods with variety of length and thickness. As for thickness, the diameter of the sample ranges from 40 to 100 nm, and the length of the nanorods is about 1–5 μm. From Fig. 3, the agglomeration phenomenon is not apparent and noticeable with a good dispersion comparatively.

3.2 SEM and mapping of nanothermites

Fig. 4 shows the SEM images of nanothermites. Fig. 4(a) is the sample I_{00} Al/MnO_2 nanothermite without $KClO_4$. The spherical particles are Al nanoparticles, and the nanorods are synthesized MnO_2. From Fig. 4(a), it is found that electrospray method could effectively reduce the agglomeration behaviour of nano powder to some extent. In Fig. 4(b)–(d), a large number of Al nanoparticles and MnO_2 nanorods directly adhere to the surface of the $KClO_4$ crystals. Namely, $KClO_4$ crystals, irregular blocks in Fig. 4, are wrapped by nanopowders, which could increase contact area of the reaction between fuel and oxides.

In order to test the distribution of the components in those nanothermites, the Mapping tests were introduced. As shown in Fig. 5, the green scatter diagram is on behalf of the Al nanoparticles, and the purple one is Mn element distribution, which represents the MnO_2 nanorods. The golden scatter diagram and blue scatter diagram, the K element and Cl element, respectively, represent the distribution of $KClO_4$ together. The Al nanoparticles and MnO_2 nanorods are evenly distributed. As for $KClO_4$, with the increase of mass fraction, the number of golden and blue points increases gradually.

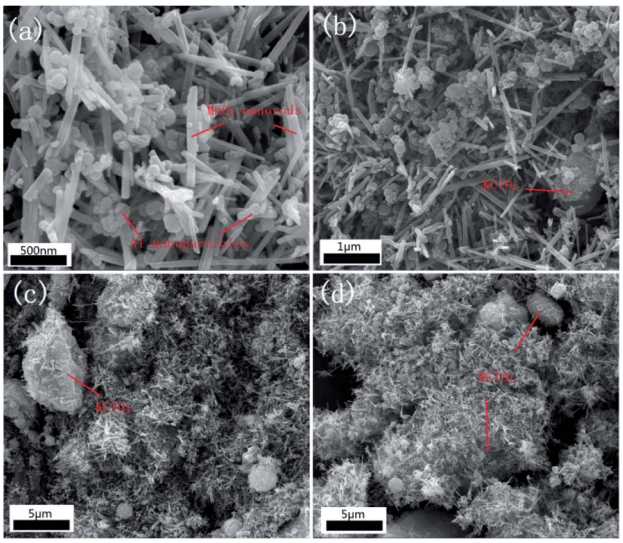

Fig. 4 SEM images of nanothermites samples (a) I_{00} Al/MnO_2 nanothermite, (b) II_{10} Al/MnO_2 nanothermite/10 wt% $KClO_4$, (c) III_{20} Al/MnO_2 nanothermite/20 wt% $KClO_4$, (d) IV_{30} Al/MnO_2 nanothermite/30 wt% $KClO_4$.

3.3 Thermal properties analysis

The TG-DSC curve of the pure $KClO_4$ and nanothermites samples at a heating rate of 20 °C min^{-1} are shown in Fig. 6. In Fig. 6(a), clearly, an endothermic peak appears at about 302 °C which corresponded to the phase change process of $KClO_4$, from rhombic to cubic structure.[22] There is a combination of endothermic and exothermic peaks at the temperature range from 590 °C to 650 °C. The endothermic peak is at about 600 °C, indicating the process of $KClO_4$ melting, and then the thermal decomposition of $KClO_4$ happens with a sharp exothermic peak at about 620 °C. At the same time, there is a sharp drop in mass of about 50% due to the gaseous oxygen release.

To figure out the catalysis of MnO_2 nanorods in $KClO_4$ system, the 80 wt% $KClO_4$/20 wt% MnO_2 mixture were prepared by ultrasonic dispersion method, and then the TG-DSC tests were carried out at same condition as shown in Fig. 6(b). Although the MnO_2 nanorods as a kind of catalyzer has no effect on its phase change, still at about 302 °C, MnO_2 nanorods could greatly reduce the temperature of melting and thermal

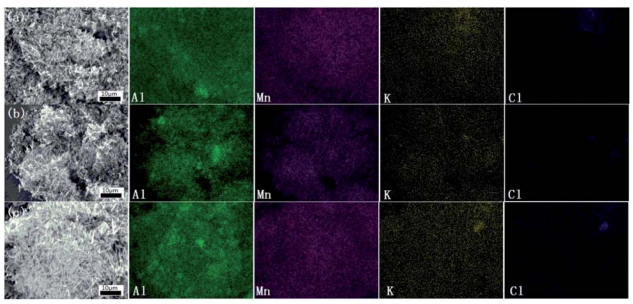

Fig. 5 Mapping of nanothermites sample (a) II_{10} Al/MnO_2 nanothermite/10 wt% $KClO_4$, (b) III_{20} Al/MnO_2 nanothermite/20 wt% $KClO_4$, (c) IV_{30} Al/MnO_2 nanothermite/30 wt% $KClO_4$.

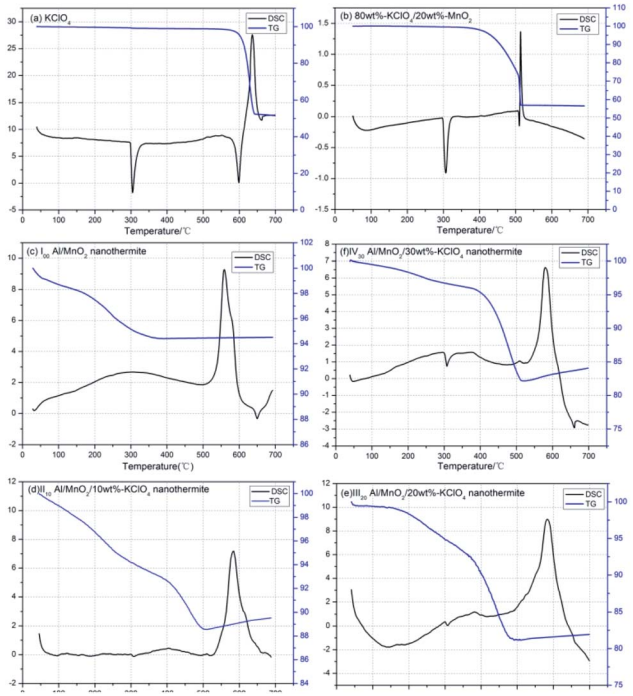

Fig. 6 TG-DSC curves of pure component and nanothermites (a) pure $KClO_4$, (b) 80 wt% $KClO_4$/20 wt% MnO_2, (c) I_{00} Al/MnO_2 nanothermite, (d) II_{10} Al/MnO_2 nanothermite/10 wt% $KClO_4$, (e) III_{20} Al/MnO_2 nanothermite/20 wt% $KClO_4$, (f) IV_{30} Al/MnO_2 nanothermite/30 wt% $KClO_4$.

decomposition, about 90 °C. As TG curve in Fig. 6(b), remarkably, the mass starts to reduce slowly at about 400 °C before melting point, and the peaks area of melting and thermal decomposition become small but sharp, which means that a few $KClO_4$ even decomposes directly at solid state. When temperature rise to 500 °C, the $KClO_4$ melts down and thermally decomposes soon. At same time, the mass is lost pretty quickly. In summary, the MnO_2 nanorods could make a significant difference to the melting and thermal decomposition of $KClO_4$.

In Fig. 6(c), the TG curve of Al/MnO_2 nanothermite goes down slowly, about 5.5% mass loss, before temperature rises to 350 °C. Based on previous reports,[29] some residual solvent are removed from the nanothermite, including the adsorb and structural water, residual ethanol. As is known to all, it is universal for nanomaterials to adsorb some water from air, especially the hydrothermal synthesized MnO_2 nanorods. In the DSC curve, an obvious exothermic peak appears at 560 °C with 1037.6 J g^{-1}, and then a small endothermic peak at about 660 °C is the melting of residual Al nanoparticles.

In the next step, the nanothermites with different mass fraction addition of $KClO_4$ were tested by TG-DSC, as shown in Fig. 6(d)–(f). All of samples have small endothermic peak at 300 °C due to phase change of $KClO_4$, which means that MnO_2 nanorods or Al nanoparticles would not catalyze the phase change at all, and as for TG curves before 350 °C, they are same to the results of Al/MnO_2 nanothermite because of the desorption of solvents on the surfaces. But it is noticeable that there is an inflection point near 400 °C in each of three TG curves. The rate of mass loss is obviously accelerating in the temperature

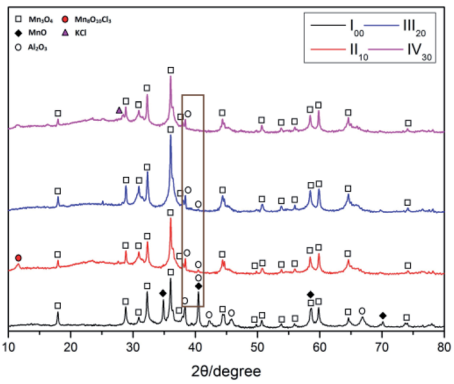

Fig. 7 XRD pattern of reaction products.

range of 390 °C–500 °C because of thermal decomposition of $KClO_4$ with gaseous oxygen release under MnO_2 nanorods catalysis. But the main exothermic peaks do not appear in this temperature range but at about 580 °C. Besides, in this temperature range from Fig. 6(d), the mass loss is about 4%, and there are 10% and 12% mass loss in Fig. 6(e) and (f), respectively. According to the results of thermal decomposition mass loss in Fig. 6(a), the decomposition process of $KClO_4$ will lead to near 50% mass loss. An approximate calculation shows that all of $KClO_4$ will decompose before the main exothermic thermite reaction, and MnO_2, as a kind of catalyzer in decomposition of $KClO_4$, is still MnO_2. Namely, to some extent, $KClO_4$ will not involve into main exothermic thermite reaction between Al and MnO_2 directly. Besides, in fact, the main exothermic peaks in Fig. 6(d)–(f) are lagging a little bit, about 20 °C. From the above, the addition of $KClO_4$ seems to have a little negative effect on the thermite reaction in Al/MnO_2 nanothermite system even though $KClO_4$ is commonly used as pyrotechnic additive and compositions to support combustion.

3.4 Analysis of reaction products

After TG-DSC tests, the residues are collected and tested by XRD to analyze the phase of reaction products. The reactants are MnO_2, Al and $KClO_4$. Therefore, the Mn, Al, O, K and Cl are set as the possible elements in residues. Clearly, the main compositions in all of residues are Mn_3O_4. Besides, the MnO and Al_2O_3 are the other compositions in residues of Al/MnO_2 nanothermite (I_{00}). As the mass fraction of $KClO_4$ increases, the crystallinity of Al_2O_3 decreases drastically and the MnO composition just disappears directly, as shown in brown box in Fig. 7. But there is a characteristic peak of $Mn_8O_{10}Cl_3$ at 11.6° in XRD pattern of residue of Al/MnO_2/10 wt%-$KClO_4$ nanothermite (II_{10}). Theoretically, due to the thermal decomposition, the KCl will be generated from $KClO_4$. In fact, only the Al/MnO_2/30 wt%-$KClO_4$ nanothermite (IV_{30}) sample detects the characteristic peak of KCl. Namely, the amount of crystallization of KCl might be very small.

3.5 Activation energy

According to the theoretical background of Kissinger method,[30,31] the TG-DSC tests were carried out under different

Table 2 The parameters of peak temperatures at different heating rates

Samples	Formulas	Heating rate/K min^{-1}	T_{peak}/°C	T_{peak}/K
I_{00}	Al/MnO_2	5	538.3	811.4
		10	542.1	815.2
		15	551.1	824.2
		20	559.0	832.1
II_{10}	Al/MnO_2/	5	541.4	814.5
	10 wt% $KClO_4$	10	569.8	842.9
		15	571.6	844.7
		20	583.1	856.2
III_{20}	Al/MnO_2/	5	544.8	817.9
	20 wt% $KClO_4$	10	562.2	835.3
		15	571.8	844.9
		20	584.6	857.7
IV_{30}	Al/MnO_2/	5	544.3	817.4
	30 wt% $KClO_4$	10	562.2	835.3
		15	571.1	844.2
		20	581.3	854.4

heating rates in a range from room temperature to 700 °C, and the parameters of peak temperatures are listed in Table 2. These parameters clearly demonstrate that the peak temperatures of nanothermites reaction are affected by the heating rates and are increased gradually with the rise of heating rates.

Fig. 8 shows the results of fitting linear, and Table 3 demonstrates that the kinetic parameters of the thermal reaction of the nanothermites. The absolute values of correlation coefficient are all greater than 0.96. The activation energy of I_{00} sample is calculated about 342.03 kJ mol^{-1} while the value of II_{10} sample is merely about 175.77 kJ mol^{-1} when the $KClO_4$ is added 10 wt%. When the mass fractions of $KClO_4$ rise to 20 wt% and 30 wt%, the activation energy will increase a little, with 196.69 kJ mol^{-1} and 207.77 kJ mol^{-1}, respectively. Namely, the addition of $KClO_4$ could significantly reduce the activation energy of the nanothermite system by up to 48.8%.

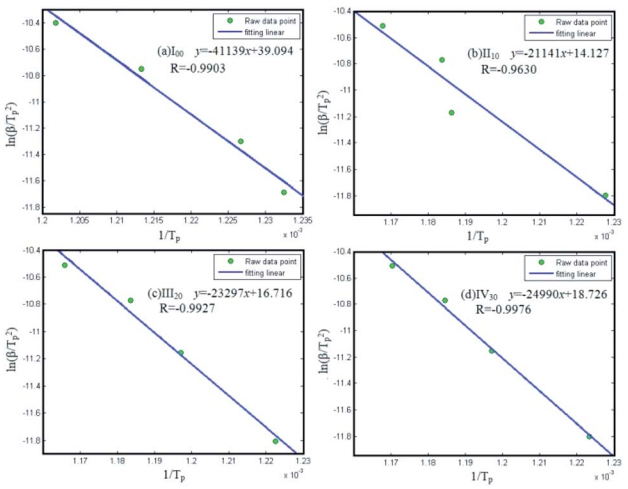

Fig. 8 Plots of $\ln(\beta/T_p^2)$ *versus* $1/T_p$ for the nanothermites (a) I_{00} Al/MnO_2 nanothermite, (b) II_{10} Al/MnO_2 nanothermite/10 wt% $KClO_4$, (c) III_{20} Al/MnO_2 nanothermite/20 wt% $KClO_4$, (d) IV_{30} Al/MnO_2 nanothermite/30 wt% $KClO_4$.

Table 3 Kinetic parameters of the thermal reaction of the nanothermites

Samples	Formulas	E_a/kJ mol^{-1}	Correlation coefficient
I_{00}	Al/MnO_2	342.03	−0.9903
II_{10}	Al/MnO_2/10 wt% $KClO_4$	175.77	−0.9630
III_{20}	Al/MnO_2/20 wt% $KClO_4$	196.69	−0.9927
IV_{30}	Al/MnO_2/30 wt% $KClO_4$	207.77	−0.9976

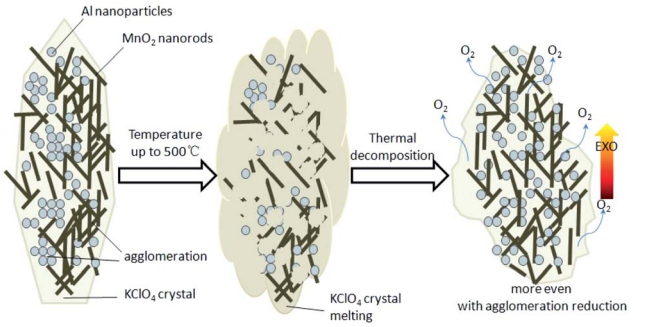

Fig. 9 Schematic diagram of change process.

According to the activation energy calculation results, there are several possible reasons as follow. Firstly, before the thermite reaction occurs, the $KClO_4$ melts first and it could wraps up nanothermites components, including the agglomerations, and then the thermal decomposition of $KClO_4$ occurs dramatically and sharply with lots of gaseous oxygen release, which could disruptive the agglomeration of Al nanoparticles and MnO_2 nanorods. Namely, to some extent, this process is equivalent to dispersing the nanothermite system again more even, just like secondary mix. Besides, the amount of gaseous oxygen release will be good for the thermite exothermic reaction, which has the effect of supporting combustion, as shown in Fig. 9. Thirdly, according to the TG-DSC results, the process of $KClO_4$ thermal decomposition is exothermic, and the main thermite reaction occurs next, which could be a kind of pre-ignition. Therefore, the activation energy of system is reduced by about 48.8% for the above possible reasons.

3.6 Onset combustion tests

The combustion properties of samples were ignited by heating wire experiments and recorded by high-speed photography. The diameter of heating wire was 0.1 mm. The 20 mg samples were ignited by a rapid heating wire at a current of 1 A. The high-speed photography took 20 000 pictures per second. In Fig. 10, when the samples are just ignited and fired, we set it as the starting time, denoted as 0 μs. The next photo is 50 μs later. At about 1 ms later, the intensity of combustion reaches the top with extremely bright fire. And then the fire begins to weaken and reduce gradually. At the same time, noticeably, the combustion energy of samples is concentrated during the ignition and burning processes with only a few sparks flying away.

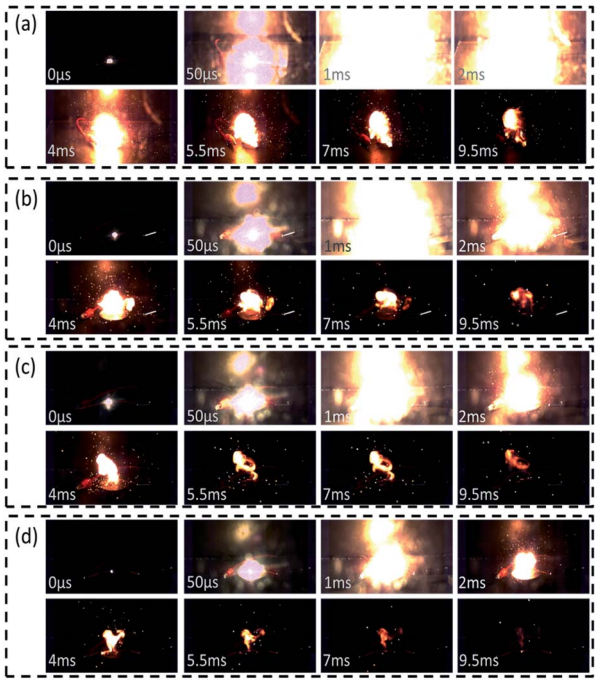

Fig. 10 Onset combustion tests of samples recorded by high-speed photography, (a) I_{00} Al/MnO_2 nanothermite, (b) II_{10} Al/MnO_2 nanothermite/10 wt% $KClO_4$, (c) III_{20} Al/MnO_2 nanothermite/20 wt% $KClO_4$, (d) IV_{30} Al/MnO_2 nanothermite/30 wt% $KClO_4$.

Comparatively, as the mass fraction of $KClO_4$ increases, the intensity of flames decreases gradually. At 1 ms, the flame of I_{00} sample almost fills the whole photo while the flame of IV_{30} sample takes up only a third of the photo. At 2 ms, the difference between the flames of I_{00} and IV_{30} samples is much more striking. Remarkably, at 9.5 ms, the flame of I_{00} sample is still clear and strong while that of IV_{30} sample is extinguished and disappeared. As for II_{10} and III_{20} samples, the decreasing trend of size of flames is also obvious.

Although the mass fraction of $KClO_4$ from 10 wt% to 30 wt% could reduce the content of Al/MnO_2 nanothermite, which will reduce the thermite reaction time to some extent, the addition of $KClO_4$ will also significantly increase the combustion rate of the samples due to its combustibility.

4 Conclusions

In this paper, the effect of $KClO_4$ on Al/MnO_2 nanothermites system was studied. The Al nanoparticles/MnO_2-nanorods nanothermites with various mass fraction of $KClO_4$ (from 0 wt% to 30 wt%) were prepared by electrospray method. According to the SEM and Mapping results, the distribution of nanothermite components was homogeneous on the surface of $KClO_4$ block. All of $KClO_4$ would be decomposed first before the thermite reaction occurred from the results of TG-DSC analysis. As for main exothermic peak of thermite reaction, the addition of $KClO_4$ had no directly positive effect on the heat release. Even worse, the main exothermic peaks with different mass fraction of $KClO_4$ were lagging a little bit, about 20 °C. The residues were collected and tested by XRD, and the main phase was Mn_3O_4. However, the introduced $KClO_4$ could drastically decrease the systematic activation energy by up to 48.8%. The possible reasons and mechanism of the effect of $KClO_4$ were analyzed. Due to the thermal decomposition, the nanothermites components are mixed more evenly without obvious agglomerations. Also, the process of $KClO_4$ thermal decomposition is exothermic, which could be a kind of pre-ignition. In the end, the onset combustion tests were carried out and recorded by high-speed photography. Clearly, the nanothermites samples with $KClO_4$ additive have much higher combustion rates with the sacrifice of heat energy, which is corresponding with the results of TG-DSC.

Conflicts of interest

The authors declare that there is no conflict of interest regarding the publication of this paper.

Acknowledgements

This work was supported by the National Natural Science Foundation, project no. 51704302, and was also supported by China Scholarship Council.

Notes and references

1 D. Spitzer, M. Comet, C. Baras, *et al.*, Energetic nanomaterials: opportunities for enhanced performances, *J. Phys. Chem. Solids*, 2010, **71**, 100.
2 C. Rossi, K. Zhang, D. Esteve, P. Alphonse, *et al.*, Nanoenergetic Materials for MEMS: A Review, *J. Microelectromech. Syst.*, 2007, **16**, 919.
3 N. H. Yen and L. Y. Wang, Reactive Metals in Explosives, *Propellants, Explos., Pyrotech.*, 2012, **37**, 256.
4 C. Rossi, A. Esteve and P. Vashishta, Nanoscale energetic materials, *J. Phys. Chem. Solids*, 2010, **71**, 57.
5 K. S. Martirosyan, Nanoenergetic Gas-Generators: principles and applications, *J. Mater. Chem.*, 2011, **21**, 9400.
6 X. Hu, X. Liao, L. Xiao, X. X. Jian and W. L. Zhou, High-Energy Pollen-Like Porous Fe_2O_3/Al Thermite: Synthesis and Properties, *Propellants, Explos., Pyrotech.*, 2016, **40**, 867.
7 S. Yan, G. Jian and M. R. Zachariah, Electrospun nanofiber-based thermite textiles and their reactive properties, *ACS Appl. Mater. Interfaces*, 2012, **4**, 6432.
8 S. G. Hosseini, A. Sheikhpour, M. H. Keshavarz and S. Tavangar, The effect of metal oxide particle size on the thermal behavior and ignition kinetic of Mg-CuO thermite mixture, *Thermochim. Acta*, 2016, **626**, 1.
9 Y. Wang, X. L. Song, W. Jiang, G. D. Deng, *et al.*, Mechanism for thermite reactions of aluminum/iron-oxide nanocomposites based on residue analysis, *Trans. Nonferrous Metals Soc. China*, 2014, **24**, 263.
10 Q. Nguyen, C. Huang, M. Schoenitz, K. T. Sullivan and E. L. Dreizin, Nanocomposite thermite powders with improved flowability prepared by mechanical milling, *Powder Technol.*, 2018, **327**, 368.

11 S. M. Umbrajkar, S. Seshadri, M. Schoenitz, V. K. Hoffmann and E. L. Dreizin, Aluminum-rich Al-MoO_3 nanocomposite powders prepared arrested reactive milling, *J. Propul. Power*, 2008, **24**, 192.
12 D. K. Kim, J. H. Bae, M. K. Kang and H. J. Kim, Analysis on thermite reactions of CuO nanowires and nanopowders coated with Al, *Curr. Appl. Phys.*, 2011, **11**, 1067.
13 Y. Ohkura, S. Y. Liu, P. M. Rao and X. Zheng, Synthesis and ignition of energetic CuO/Al core/shell nanowires, *Proc. Combust. Inst.*, 2011, **33**, 1909.
14 A. Bacciochini, M. I. Radulescu, M. Yandouzi, G. Maines, J. J. Lee and B. Jodoin, Reactive structural materials consolidated by coldspray: Al–CuO thermite, *Surf. Coat. Technol.*, 2013, **226**, 60.
15 K. Zhang, C. Rossi, P. Alphonse, C. Tenailleau, *et al.*, Integrating Al with NiO nano honeycomb to realize an energetic material on silicon substrate, *Appl. Phys. A: Mater. Sci. Process.*, 2008, **94**, 957.
16 H. Wang, M. R. Zachariah, L. Xie and G. Rao, Ignition and Combustion Characterization of Nano-Al-AP and Nano-Al-CuO-AP Micro-sized Composites Produced by Electrospray Technique, *Energy Procedia*, 2015, **66**, 109.
17 H. Wang, G. Jian, G. C. Egan and M. R. Zachariah, Assembly and reactive properties of Al/CuO based nanothermite microparticles, *Combust. Flame*, 2014, **161**, 2203.
18 A. Jaworek, Micro- and nanoparticle production by electrospraying, *Powder Technol.*, 2007, **176**, 18.
19 N. Bock, M. A. Woodruff, D. W. Hutmacher, *et al.*, Electrospraying, a reproducible method for production of polymeric microspheres for biomedical applications, *Polymers*, 2011, **3**, 131.
20 J. Marsalek, J. Chmelar, J. Pocedic and J. Kosek, Morphological and electrochemical study of Mn_xO_y nanoparticle layers prepared by electrospraying, *Chem. Eng. Sci.*, 2015, **123**, 292.
21 S. H. Fischer and M. C. Grubelich, A survey of combustible metals, thermites, and intermetallics for pyrotechnic applications, *AIAA J.*, 1996, DOI: 10.2514/6.1996-3018.
22 M. Fathollahi and H. Behnejad, A comparative study of thermal behaviors and kinetics analysis of the pyrotechnic containing Mg and Al, *J. Therm. Anal. Calorim.*, 2015, **120**, 1483.
23 X. Kang, J. Zhang, Q. Zhang, K. Du and Y. Tang, Studies on ignition and afterburning processes of $KClO_4$/Mg pyrotechnics heated in air, *J. Therm. Anal. Calorim.*, 2012, **109**, 1333.
24 F. Yang, X. L. Kang, J. S. Luo, *et al.*, Laser emission from flash ignition of Zr/Al nanoparticles, *Opt. Express*, 2017, **25**, A932.
25 F. Yang, X. L. Kang, J. S. Luo, Z. Yi and Y. J. Tang, Preparation of core–shell structure $KClO_4$@Al/CuO Nanoenergetic materials and enhancement of thermal behavior, *Sci. Rep.*, 2017, **7**, 3730.
26 B. Clark, J. McCollum, M. L. Pantoya, R. J. Heaps and M. A. Daniels, Development of flexible, free-standing, thin films for additive manufacturing and localized energy generation, *AIP Adv.*, 2015, **5**, 087128.
27 J. S. Lee and C. K. Hsu, The DSC studies on the phase transition decomposition and melting of potassium perchlorate with additives, *Thermochim. Acta*, 2001, **367**, 367.
28 K. Kishore and M. R. Sunitha, Effect of transition metal oxides on decomposition and deflagration of composite solid propellant systems: a survey, *AIAA J.*, 1979, **17**, 1118.
29 R. T. Yang and M. Steinberg, Reaction kinetics and differential thermal analysis, *J. Phys. Chem.*, 1976, **80**, 965.
30 P. E. Sánchez-Jiménez, J. M. Criado and L. A. Pérez-Maqueda, Kissinger kinetic analysis of data obtained under different heating schedules, *J. Therm. Anal. Calorim.*, 2008, **94**, 427.
31 W. M. Dose and S. W. Donne, Manganese dioxide structural effects on its thermal decomposition, *Mater. Sci. Eng., B*, 2011, **176**, 1169.